

## A Fast-Locking, Low-Jitter Pulsewidth Control Loop for High-Speed ADC

Zhangming Zhu, Maliang Liu, Jingyu Wang, and Yintang Yang

**Abstract**—A fast-locking, high-precision, and low-jitter pulsewidth control loop (PWCL) for high-speed high-resolution analog-to-digital converter is presented. Only through controlling the delay of rising edge to adjust duty cycle, the clock jitter could be suppressed greatly. An improved charge pump with a follower circuit and self-biased loop was designed to decrease the voltage ripples for higher accuracy and lower jitter. A startup circuit was adopted to enable the pulsewidth control loop lock rapidly. With the SMIC 0.18  $\mu\text{m}$  3.3 V CMOS process, the simulation and measured results show that within 180 ns the PWCL can lock the clock duty cycles for the accuracy of  $50 \pm 1\%$  with 10%~90% input duty cycle from 50 to 550 MHz. The rms-jitter is 73 fs at 250 MHz. The active area is about 0.023  $\text{mm}^2$ .

**Index Terms**—Charge pump, clock jitter, CMOS, pipelined analog-to-digital converter (ADC), pulsewidth control loop (PWCL).

### I. INTRODUCTION

To meet the demand of high-speed CMOS VLSI circuits, many high-speed analog-to-digital converters (ADCs) adopt double data rate technology [1]–[12] to get large data throughput. Compared with other ADCs, pipelined ADCs have an abroad application in many electronic systems with merits of high speed, good precision, and low power dissipation. In the design of pipelined ADCs, the jitter and accuracy of the system clock become more a concern as both ADC resolution and analog input frequency increase [10]. So the system clock optimization for low-jitter and high accuracy can be both challenging and rewarding. The pulsewidth control loop (PWCL) mechanism is developed to solve this problem perfectly.

The conventional PWCL [3] that adjusts the duty cycle by controlling the delay of rising and falling edges has a high jitter and long locking time. The fast-locking PWCL [4] modified from the conventional PWCL can achieve a fast locked and presentable output duty cycle. But it requires an exact 50% duty cycle of the clock signal and a voltage-difference-to-digital converter, which costs larger chip size and more power consumption. Another PWCL [10] using second-order passive loop filter has a lower power consumption, but chip area and loop stability are unavoidable problems.

In this brief, a new PWCL circuit is proposed, which introduce a startup circuit to obtain a fast locking. Moreover, an improved charge pump is used to reduce the ripple voltage for higher accuracy and lower jitter. The clock jitter could be greatly suppressed and the complication of circuit could also be reduced only through controlling the delay of rising edge to adjust duty cycle. The architecture of the proposed PWCL is discussed in Section II. The system analysis and design are discussed in Section III. The experimental results are illustrated in Section IV.

Manuscript received March 9, 2013; revised August 27, 2013; accepted September 4, 2013. This work was supported in part by the National Natural Science Foundation of China under Grant 61234002, Grant 61322405, Grant 61306044, and Grant 61376033, in part by the National High-tech Program of China under Grant 2012AA012302 and Grant 2013AA014103, and in part by the Ph.D. Programs Foundation of the Ministry of Education of China under Grant 20120203110017.

The authors are with the School of Microelectronics, Xidian University, Xi'an 710071, China (e-mail: zhangmingzhu@xidian.edu.cn; liumalianghy@163.com; 7144670\_yu@sina.com; ytyang@xidian.edu.cn).

Color versions of one or more of the figures in this paper are available online at <http://ieeexplore.ieee.org>.

Digital Object Identifier 10.1109/TVLSI.2013.2281318

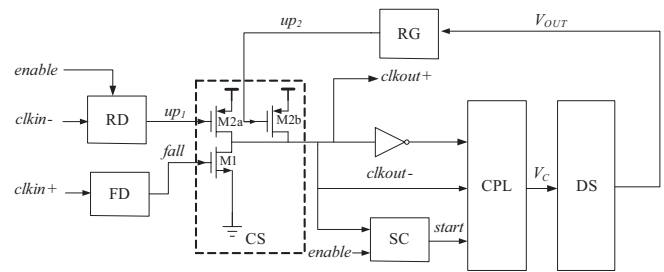


Fig. 1. Proposed PWCL architecture.

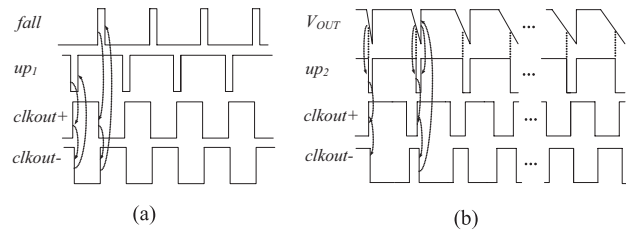


Fig. 2. (a) Duty-cycle tracking mode. (b) Duty-cycle correction mode different mode of proposed PWCL.

### II. ARCHITECTURE OF PROSPOED PWCL

The proposed PWCL architecture is shown in Fig. 1. It includes the control Stage (CS), charge pump loop (CPL), delay stage (DS), startup circuit (SC), rising edge generator (RG), rising edge differentiator (RD), and falling edge differentiator (FD). In different applications, the PWCL is used in either the duty-cycle tracking mode or the duty-cycle correction mode. The timing diagrams for duty-cycle tracking mode and duty-cycle correction mode are shown in Fig. 2(a) and (b). The choice for mode is controlled by the signal enable. In the duty-cycle tracking mode, the charge pump loop, delay stage, startup circuit, and rising edge generator do not work so as to reduce the power dissipation, and the output duty cycle is maintained to be the same as the input duty cycle. In the duty-cycle correction mode with the rising edge differentiator off, the falling edge differentiator generates a pulse at every rising edge of the input signal, while the pulse has specific width, equal to the transmission delay of several inverters [11]. The pulse triggers the control stage to generate the falling edge of output clock. With a fixed-delay falling edge, the PWCL initialized by startup circuit has the biggest duty cycle in the first correction period, and then adjusts the duty cycle by controlling the delay of a low pulse, which triggers the control stage to generate the rising edge. The low pulse  $up_2$  generated from the rising edge generator is affected by the delay stage, which controlled by the voltage  $V_C$  generated from charge pump loop.

Compared with the conventional PWCL circuits which adjust duty cycle through double-edge modulating, the proposed PWCL could suppress the jitter of input clock to a half. To obtain a fast locking-time, a startup circuit is used to initialize the voltage of charge pump loop. The key circuits in the PWCL are discussed in detail below.

#### A. Charge Pump Loop

Fig. 3 shows the circuit structure of the charge pump loop, which mainly consists of an improved charge pump and low-pass filter and single-stage amplifier. The charge pump converts duty cycle into current, which charges or discharges capacitor CP of the low-pass filter. The low-pass filter changes the current signal to voltage signal  $V_{C1}$ , finishing a current-to-voltage conversion. Another function of low-pass filter is to reduce the ripples which resulting in clock jitter [6].

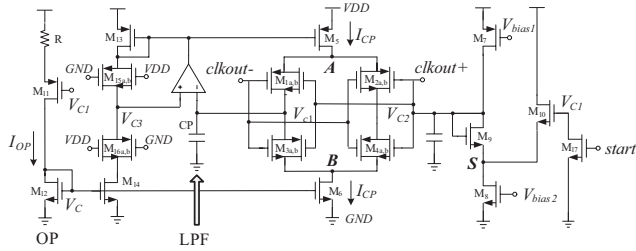


Fig. 3. Charge pump loop.

The voltage  $V_{C1}$  is applied on single-stage operational amplifier to produce a control voltage  $V_C$  to the delay stage, thereby generating delay time to change the duty cycle to the target ratio. The initial value of  $V_{C1}$  is decided by the startup circuit, and then the startup circuit won't function. During the initializing process of  $V_{C1}$ , the startup circuit generated a start signal to discharge the voltage of  $V_{C1}$ .

The ripple of control voltage  $V_C$  determines the jitter and the duty cycle error of the output clock. The performance of charge pump influences the ripple of  $V_C$  directly. Among all the nonideal factors affecting the performance of current pump, current mismatch, and charge sharing have a heavy effect.

To obtain a perfect current matching characteristic, we propose a new improved charge pump, which adopts combined charge pump and self-biasing technique to guarantee the sourcing/sinking current matching. Since the follower exists between the point  $V_{C1}$  and  $V_{C2}$ , the voltages of two points always keep the same. Meanwhile because of the feedback brought by amplifier existing in self-biasing loop, the point voltage  $V_{C3}$  is equal to  $V_{C1}$ . So  $V_{C3} = V_{C1} = V_{C2}$ . The combined charge pump structure uses the complementary signals  $clkout^+$  and  $clkout^-$  as inputs. Either the left side or the right side of the switches is turned on to charge or discharge  $V_{C1}$  and  $V_{C2}$ . The current  $I_{CP}$  always has one turn-on path, thus stabilizing the voltage of nodes *A* and *B*. So the voltages in nodes *A* and *B* can be kept nearly constant. Meanwhile through using the same size transmission gates *M1*, *M2*, *M15*, and *M3*, *M4*, *M16*, the drains of biasing MOSFET, current sink and current source in the charge pump keep the same voltage, avoiding being affected by short channel modulation, which caused the current mismatch.

In addition, using the self-biasing technique, the biasing voltage for current source/sink in charge pump is generated from current mirror loop composed by *M5*, *M6*, *M13*, and *M14*. Thus  $I_{CP} = kI_{OP}$ , where  $k$  equals the size ratio of *M5* and *M13*, *M6*, and *M14*. Self-biasing avoids the necessity for external biasing, which can require special bandgap bias circuits, by generating all of the internal bias voltages from each other so that the bias levels are completely determined by the operating conditions.

In the ordinary charge pump, charge sharing effect could cause a jump phenomenon which brings the control voltage bigger ripples, resulting in worse jitter performance and duty-cycle accuracy. This brief gives a new structure with a follower circuit between two sides of charge pump. The voltage  $V_{C1}$  is applied as input of the *M10*, while *M7* used as current source load. Diode-connected device *M9* could give a voltage level shift to the node *S*. Since *M9* and *M10* have the same size, we have  $V_{GS10} = V_{C1} - V_S = V_{TH} + V_{DSAT}$ ,  $V_{GS9} = V_{C2} - V_S = V_{TH} + V_{DSAT}$ , thus  $V_{C1} = V_{C2}$ . As a result, if all four switches turn off, the drain voltages of *M1*, *M2*, *M3*, and *M4* will be held to equal. Therefore, it won't produce the jump phenomenon in the nodes *A* and *B*. So the charge sharing problem can be eliminated.

A SMIC 0.18  $\mu\text{m}$  3.3 V CMOS Spice model is used for simulation. Fig. 3 shows the wave forms of the voltages  $V_{C1}$  and  $V_{C2}$  and  $V_C$

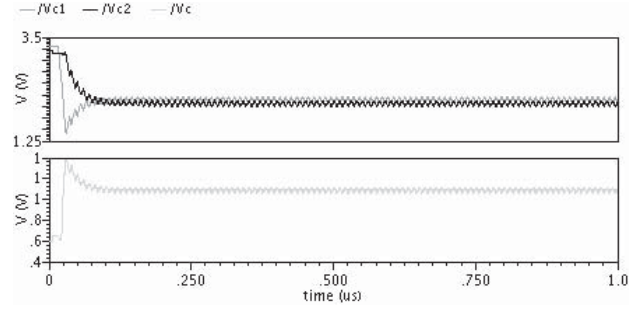
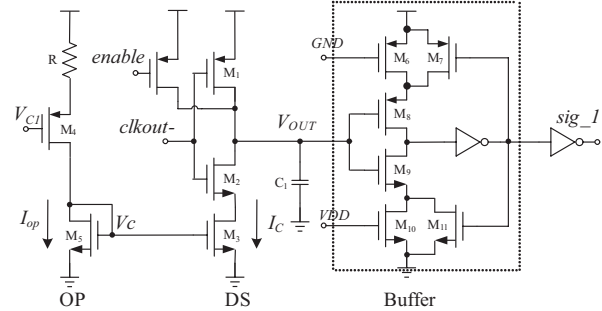

 Fig. 4. Simulations of the voltages  $V_{C1}$ ,  $V_{C2}$ , and  $V_C$  at a frequency of 100 MHz.


Fig. 5. Schematic of single-stage amplifier, delay stage, and the buffer of rising edge generator.

at a frequency of 100 MHz. Since the usage of improved charge pump, the current mismatch and charge sharing effects are suppressed greatly. The error voltage between  $V_{C1}$  and  $V_{C2}$  is reduced leading to a smaller voltage ripple at  $V_C$ , lower jitter and high duty-cycle accuracy at output clock.

### B. Single-Stage Amplifier and Delay Stage

The schematics of single-stage amplifier in charge pump loop, delay stage and buffer in rising edge generator are shown in Fig. 5. Single-stage amplifier, adopting common source with source degeneration, amplifies the input voltage  $V_{C1}$  into the control voltage  $V_C$  for driving delay stage to generate different delay time. By controlling the discharging speed of  $C_1$  in delay stage, the PWCL can adjust the duty cycle of output clock to a precise 50% duty cycle.

The delay stage consists of the inverter with  $V_C$  as control voltage, the capacitor  $C_1$ . The buffer with positive feedback generates the pulse with steeper edges, which triggers the rising edge generator to give a low-level pulse that brings the rising edge of output clock. In this circuit, we have  $I_{OP} = k_1 I_C$ , where  $I_C$  and  $I_{OP}$  represent discharging current of delay stage and current of single-stage amplifier, respectively.  $k_1$  is ratio of size parameter of *M5* and *M3*. When *M3* and *M5* have the same size, we have  $I_C = I_{OP} = V_{C1}GM$ . Where  $GM$  is transconductance of single-stage amplifier, and  $GM < 0$ , so  $I_C$  is inverse to  $V_{C1}$ . Assumed that the node voltage  $V_{OUT}$  has a drop voltage  $\Delta V_{OUT}$ , the PWCL generates the pulse which triggers the rising edge of  $clkout^+$ . So the delay time generated by delay stage in the  $n_{th}$  period can be expressed as

$$\begin{aligned}
 t &= \frac{2C_1 \Delta V_{OUT}}{I_{ctrl}} \\
 &= \frac{2C_1 \Delta V_{OUT}}{V_{C1} GM} \\
 &= \frac{2C_1 \Delta V_{OUT}}{GM(V_{initial} + \Delta V_{C1}(n-1) + \Delta T(n)kI_{OP})} \quad (1)
 \end{aligned}$$

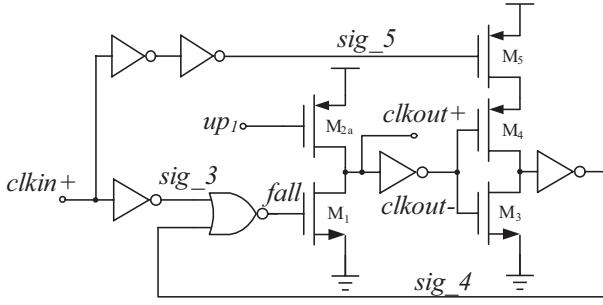


Fig. 6. Schematic of the falling edge differentiator.

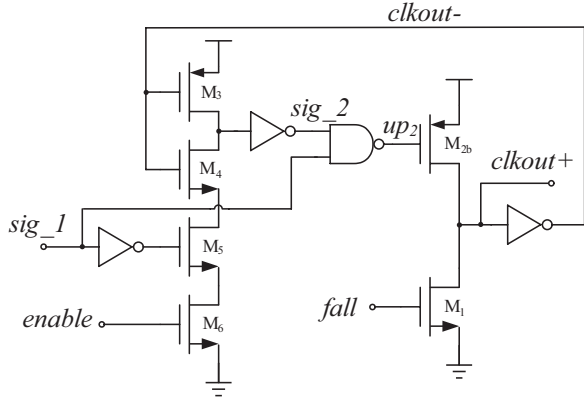


Fig. 7. Schematic of the rising edge generator.

where  $k$  is the ratio between  $I_{CP}$  and  $I_{OP}$ .  $\Delta T(n) = T_1(n) - T_2(n)$ ,  $T = T_1(n) + T_2(n)$ ,  $T_1(n)$  and  $T_2(n)$  represent the time of  $clkout^+$  is logic 1 and 0, respectively.  $V_{initial}$  is the initial voltage of the charge pump after startup circuit gives a start signal pulse.  $\Delta V_{C1}(n-1)$  is the variety of  $V_{C1}$  after  $n-1$  periods. When the PWCL is locked, the duty cycle is 50%. And  $T_1(n) = T_2(n) = T/2$ ,  $\Delta T(n) = 0$ , therefore  $V_{C1}$  maintains constant. Accordingly, the delay time is equal to  $T/2$  and the PWCL keeps stable.

### C. Rising Edge Generator, Falling Edge Differentiator, and Control Stage

The schematics of rising edge generator and falling edge differentiator are shown in Figs. 6 and 7. At every rising edge of  $clkin^+$ , the falling edge differentiator generates a high voltage pulse, which pulls down the  $clkout^+$  through using the  $clkin^+$  and the feedback signal as inputs of NOR gate. When the rising edge of  $clkin^+$  arrives,  $sig_3$  is pulled down from high voltage to low voltage. Meanwhile the  $sig_4$  is still low voltage. So the output of NOR generates a narrow high-voltage pulse, and changes the logic state of  $clkout^+$  through control stage. With the same theory, the rising edge generator generates the low-voltage pulse that triggers the control stage to pull up  $clkout^+$ , through detecting the output signal  $V_{OUT}$  of the delay stage.

The control stage of PWCL consists of  $M1$ ,  $M2a$ , and  $M2b$ . In different work modes,  $M2$  works with either  $M2a$  or  $M2b$ . In the duty-cycle tracking mode,  $M2b$  shuts down because signal  $up2$  stays high voltage. In duty-cycle correction mode,  $M2a$  shuts down because signal  $up1$  stays high voltage.

### III. LOOP ANALYSIS OF THE PROPOSED PWCL

The linear model of the proposed PWCL is shown in Fig. 8, and  $D_{in}(s)$  is the input duty cycle,  $D_{out}(s)$  is the output duty cycle,  $K_{CP}$  is the

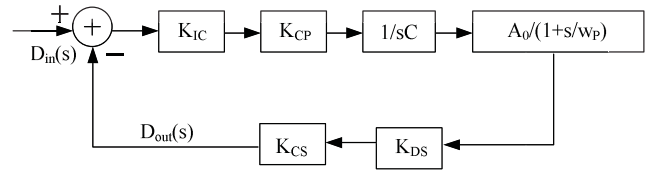


Fig. 8. Linear model of the proposed PWCL.

charge pump gain,  $A_0$  and  $w_p$  is the gain and dominant pole of the single-stage amplifier respectively,  $K_{CS}$  is the control stage gain,  $K_{DS}$  is the delay stage gain,  $K_{IC}$  is the gain of inverter, CP is the low-pass filter capacitor. Since  $w_p$  locates at very high frequency, the influence of  $w_p$  can be ignored. The locking time analysis approximates first-order system.

The closed-loop transfer function can be represented as follows:

$$H(s) = \frac{D_{out}(s)}{D_{in}(s)} = \frac{1}{s \frac{K_{IC} \times K_{CP} \times A_0 \times K_{DS} \times K_{CS}}{C} + 1}. \quad (2)$$

The step response for the first-order system can be expressed as follows:

$$\Delta D_{out}(t) = \Delta D_{out} \left[ 1 - e^{-\frac{-K_{IC} K_{CP} A_0 K_{DS} K_{CS} t}{C}} \right] \quad (3)$$

where  $\Delta D_{out}$  denotes the variety of output duty cycle in the step response. When the duty-cycle error is below 1% in 250 MHz, in the proposed PWCL,  $I_{CP} = 208 \mu A$ ,  $K_{CP} = 2I_{CP}$ ,  $K = K_{IC} A_0 K_{DS} K_{CS} = 0.96 V^{-1}$ . Considering of the demand of locking time and accuracy, the capacitor of the low-pass filter  $C = 8$  pF. After being initialized by the startup circuit, the output duty cycle changed from 25% to  $50 \pm 1\%$ , the settling time  $T_S$  can be solved from (2).

The locking time  $T_{LOCK} = T_{START} + T_S$ , where  $T_{START}$  is the pulse width of start from startup circuit. Because of the delay of startup circuit elements and input clock, in the real situation, for the different input duty cycle in different frequency, the locking time of PWCL is approximately below 180 ns when the duty cycle arrives at the accuracy of  $50 \pm 1\%$ .

### IV. EXPERIMENT RESULTS

The proposed PWCL is implemented using the SMIC 0.18  $\mu m$  3.3 V CMOS process. The proposed PWCL can modulate the input clock with 10%~90% input duty cycle from 50 to 550 MHz, and get the output clock for the accuracy of  $50 \pm 1\%$ . Fig. 9 shows the PWCL adjusts the output duty cycle to  $50 \pm 1\%$  when the input clock has different duty cycle at 500 MHz.

Fig. 10 shows the peak-to-peak and rms-jitter for the 250 MHz output clock at 640 and 73 fs through eyeDiagram analysis. With the simulation and experiment results, the proposed PWCL can operate correctly at different frequencies and duty cycles of the input clock and produce the clock with accuracy of  $50 \pm 1\%$ , and achieve fast locking and low jitter. It can satisfy the applications of the ADC with high-speed and high-precision perfectly. This circuit has finished the layout design, and through the dummy MOSFET, the mismatch has been decreased heavily. The proposed PWCL die micro-photo is shown in Fig. 11, the active area is about  $0.023 \text{ mm}^2$ .

On the comparison with other PWCLs, which have been realized, the proposed PWCL has the obvious advantages at the range of input

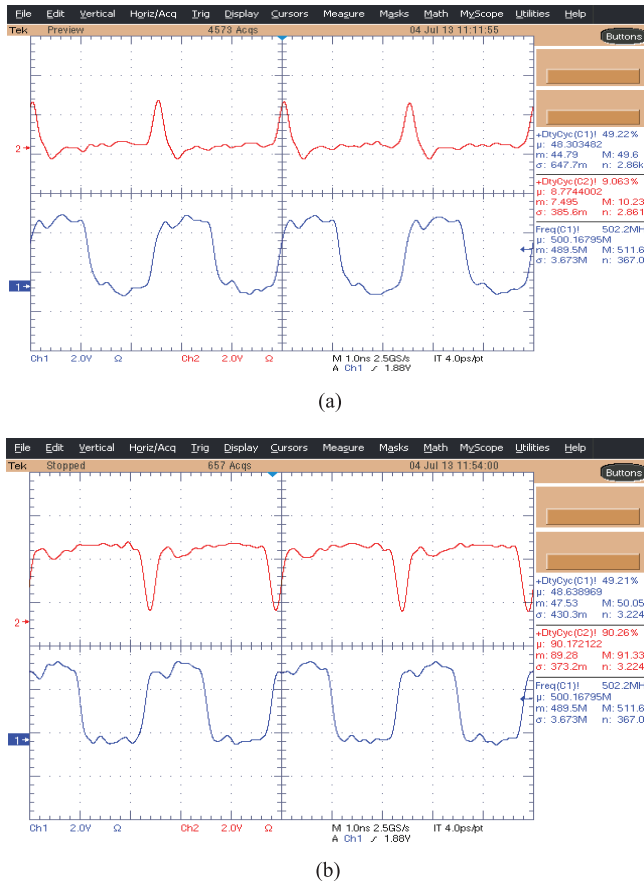


Fig. 9. (a) Frequency = 500 MHz, Clkin = 90%. (b) Frequency = 500 MHz, Clkin = 10% Frequency = 500 MHz, the output clock is 50% for the input clock in different duty cycle.

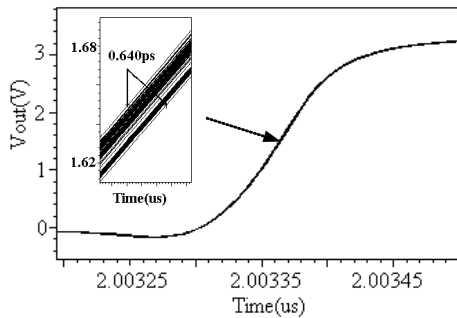


Fig. 10. EyeDiagram analysis in 250 MHz.

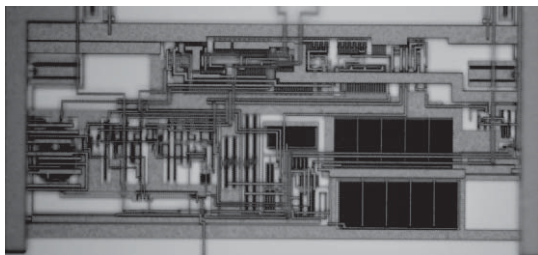


Fig. 11. Microphoto of the proposed PWCL.

clock duty cycle, locking-time and jitter characteristic and chip area. Table I presents the performance comparison of the proposed PWCL

TABLE I  
PERFORMANCE COMPARISON OF PWCLs

	This Work	[7]	[8]	[9]	[10]
Technology ( $\mu\text{m}$ )	0.18	0.18	0.18	0.18	0.18
Supply Voltage(V)	3.3	1.8	1.8	1.8	1.8
Locking Time(ns)	180	N/A	600	<36 cycles	<405
Input Duty(%)	10~90	40~60	30~70	30~70	10~80
Output Duty(%)	$50 \pm 1$	$50 \pm 1$	30~70	$50 \pm 1$	30~60
Clock Jitter	rms jitter 73fs@ 250M Hz	p-p jitter 3.2ps @1 GHz	rms jitter 1.9ps @1.3 GHz	p-p jitter 28.9ps @250 MHz	N/A
Active Area	0.023 $\text{mm}^2$	N/A	0.057 $\text{mm}^2$	0.09 $\text{mm}^2$	N/A

and the others.

## V. CONCLUSION

For the high-speed and high-resolution ADC, a fast-locking, high-precision, and low-jitter system clock has an important influence to the characteristics of the ADC. Mended from the conventional PWCL, the system presented in this brief uses the single edge to adjust the duty cycle accurately. An improved charge pump is used to reduce the jitter and error of duty cycle greatly. The locking-time is shorted by utilizing the startup circuit to initialize the charge pump voltage. The proposed PWCL can modulate the input clock with 10%~90% input duty cycle from 50 to 550 MHz, and get the output clock for the accuracy of  $50 \pm 1\%$ . The proposed PWCL can be used in various applications, especially in the high-speed and high-resolution ADC.

## REFERENCES

- [1] D. Shin, C. Kim, J. Song, and H. Chae, "A 7ps jitter 0.053mm<sup>2</sup> fast lock all-digital ADDLL with a wide range and high resolution DCC," *IEEE J. Solid-State Circuits*, vol. 44, no. 9, pp. 2437–2451, Jan. 2009.
- [2] T.-H. Lin, C.-C. Chi, W.-H. Chiu, and Y.-H. Huang, "A synchronous 50% duty-cycle clock generator in 0.35- $\mu\text{m}$  CMOS," *IEEE Trans. Very Large Scale Integr. (VLSI) Circuits Syst.*, vol. 19, no. 4, pp. 585–591, Apr. 2011.
- [3] R.-M. Weng, C.-Y. Liu, and Y.-C. Lu, "A low Jitter DLL-based pulse width control loop with duty cycle adjustment," in *Proc. IEEE Asia Pacific Conf. Circuits Syst.*, Dec. 2008, pp. 418–421.
- [4] S.-R. Han and S.-I. Liu, "A 500MHz-1.25 GHz fast-locking pulsewidth control loop with presentable duty cycle," *IEEE J. Solid-State Circuits*, vol. 39, no. 3, pp. 463–468, Feb. 2004.
- [5] K.-H. Cheng, C.-W. Su, K.-F. Chang, C.-L. Hung, and W.-B. Yang, "A high linearity and fast-locked pulse width control loop with digitally programmable output duty cycle for wide range operation," in *Proc. 32nd Eur. Solid-State Circuits Conf.*, 2006, pp. 178–181.

- [6] P. S. Rudraswamy and S. B. Duty, "Cycle correction using negative feedback loop," in *Proc. 16th Int. Conf. Mixed Design Integr. Circuits Syst.*, 2009, pp. 424–426.
- [7] S.-K. Kao and Y.-D. You, "Pulsewidth control loop with low control voltage ripple," in *Proc. Int. MultiConf. Eng. Comput. Sci.*, vol. 2, 2012, pp. 23–25.
- [8] K.-H. Cheng, C.-W. Su, and K.-F. Chang, "A high linearity, fast-locking pulsewidth control loop with digitally programmable duty cycle correction for wide range operation," *IEEE J. Solid-State Circuits*, vol. 43, no. 2, pp. 399–413, Feb. 2008.
- [9] Y.-G. Chen, H.-W. Tsao, and C.-S. Hwang, "A fast-locking all-digital deskew buffer with duty-cycle correction," *IEEE Trans. Very Large Scale Integr. (VLSI) Circuits Syst.*, vol. 21, no. 2, pp. 1–11, Feb. 2013.
- [10] M. M. Navidi and A. Abrishamifar, "A fast lock time pulsewidth control loop using second order passive loop filters," in *Proc. 19th ICEE*, 2011, pp. 1–5.
- [11] S. S. Neiman and V. Melamed-Cohen, "E, Synchronous duty cycle correction circuit," in *Proc. VLSI-SoC*, 2010, pp. 96–100.
- [12] C.-C. Chung, D. Sheng, and S.-E. Shen, "A wide-range all-digital duty-cycle corrector with output clock phase alignment in 65nm CMOS technology," *IEICE Electron. Expr.*, vol. 8, no. 15, pp. 1245–1251, 2011.